The 1st International Conference of Health Institut Kesehatan Mitra Bunda 2024
Volume 2024
http://dx.doi.org/10.11594/nstp.2024.4304

NST Proceedings
OPEN ACCESS

Conference Paper

Viroinformatic Study of Star Anise (*Illicium verum*) as Mpro Inhibitor in SARS-CoV-2 Infection

Steven Arianto[1]*, Milda Rianty Lakoan[2], Varda Arianti[2]

[1]Department of Medical Laboratory Technology, Hermina Institute of Health, Jakarta 13320, Indonesia
[2]Department of Pharmacy, Hermina Institute of Health, Jakarta 13320, Indonesia

Corresponding author:
E-mail:
steven.arianto92@gmail.com

ABSTRACT

The spread and infection of SARS-CoV-2 towards the end of 2019 started the COVID-19 outbreak. Additionally, the antiviral medications that are still missing. Spices were among the many traditional medicines used in Indonesia. This research aims to find possible bioactive compounds in star anise with antiviral qualities to treat COVID-19 against SARS-CoV-2 proteases through the in-silico approach. Samples were obtained from the Protein Data Bank (PDB) and PubChem (NCBI, USA). Then, drug-likeness analysis was performed on the SCFBIO web server using the Lipinski rule of five. Additionally, the binding activity and molecular interaction by PoseView web server and PyMol software v2.4.1 (Schrödinger, Inc., USA) were determined by the blind docking approach using PyRx 0.8 software. Using Lipinski's rule of five, the eighty-one bioactive chemicals in star anise were examined to see how similar they were to therapeutic compounds. The molecular docking procedure was then executed using PyMOL and PyRx 0.8 (Virtual Screening Tool) and its interaction with Mpro protein. Methylphenyl has been revealed to have the lowest binding energy for Mpro SARS-CoV-2 and great potential as an inhibitor of SARS-CoV-2 viral replication based on the comprehensive research conducted on these bioactive compounds. However, since the results are only computational, a wet lab study is required for validation. Of 38 drug-like bioactive chemicals of star anise, only methylphenyl has the lowest binding affinity, which can bind and function as inhibitor of the Mpro protease enzyme. A can obstruct the SARS-CoV-2 virus's reproduction. As a result, the SARS-CoV-2 virus cannot assemble its genetic material, capsids, and other body components. Viral replication can be stopped to lower the amount of genetic material copied from the virus.

Keywords: Antiviral, Illicium verum, in silico, Mpro, SARS-CoV-2

Introduction

These days, COVID-19 is the sickness that threatens the planet in many different spheres of life. Experts refer to this illness as the "disease of a thousand faces" because of its propensity to manifest in several variants. A novel kind of Acute Respiratory Infection in Humans (SARS-CoV-2)—an infectious pathogen member of the Beta coronaviruses (Beta-CoVs) family—caused this illness. Numerous interactions, including those between people and other living things, can result in the propagation of this virus (Ansori et al., 2020). A COVID-19 infection manifests as a persistent cough, trouble breathing, and a five-day incubation period for a chest infection (38.1–39 °C). On the other hand, in extreme situations, it can result in bronchitis, a serious respiratory condition, kidney failure, and even death (Kocaadam & Şanlier, 2017).

Two protease proteins, Plpro and main protease (Mpro), encode coronavirus polyproteins (Kandeel & Al-Nazawi, 2020). The 11 cleavage sites of the Mpro protein make it an enzyme essential to the transcription and replication of viral proteins. The virus will then die due to this

How to cite:
Arianto, S., Lakoan, M. R., & Arianti, V. (2024). Viroinformatic study of star anise (*Illicium verum*) as mpro inhibitor in SARS-CoV-2 infection. *The 1st International Conference of Health Institut Kesehatan Mitra Bunda 2024*. NST Proceedings. pages 20-26. doi: 10.11594/ nstp.2024.4304

enzyme's inhibition of activity, which will prevent RNA replication. In addition, humans do not contain this sort of protease enzyme. Under such circumstances, Mpro inhibitors won't harm people by being poisonous. For this reason, according to Zhang et al. (2020), this enzyme is one of the most significant COVID-19 antiviral therapeutic candidates.

Plants with active medicinal chemicals that have anti-fungal, anti-bacterial, and anti-viral properties are one of the many strategies that have been tried to manage and even lower the number of COVID-19 cases. The fruit of the star anise plant contains about 81 active chemicals, the majority of which are alkaloids, flavonoids, essential oils, and tannins (Patra et al., 2020). Flavonoid groups, such as kaempferol, can inhibit the rabies virus's reproduction ability (Chen et al., 2021). One bioinformatics technique called molecular docking is frequently used to assess the potential of bioactive compounds from organisms that can inhibit the spread of viruses (Umesh et al., 2020; Shaghaghi, 2020; ul Qamar et al., 2020). This technique is employed to forecast the interactions between active substances (ligands) and proteins (receptors) (Earlia et al., 2019). Moreover, a complex modeling system called molecular dynamics is utilized to investigate molecular docking results' chemical and physical elements (Liguori et al., 2020). This work aims to employ molecular docking to determine the effectiveness of the chemicals in the *I. verum* plant in inhibiting COVID-19, intending to provide reference data for future investigations.

Material and Methods

Ligand preparation

To get samples in the structural data format (.sdf), 55 compounds of *Illicium verum* were assembled from the PubChem database (Table 1). Energy reduction was then carried out, and.sdf samples were transformed into .pdb format. Energy reduction was carried out for each molecule using the Python Prescription 0.8 (PyRx; Virtual Screening Tool) software, and it was finished by using OpenBabel with the default parameters. PyRx is a free program that works well for all processes and can be used for virtual screening from any platform.

Protein preparation

The 3C-like-protease-3CLpro, also known as the SARS-CoV-2 major protease (Mpro), is a therapeutic target that can be obtained and downloaded from the Protein Data Bank website (http://www.rcsb.org//pdb). The protein code PDB: 6LU7 may be used to get the three-dimensional SARS-CoV-2 crystal structure in SDF format from the Protein Data Bank website. Using PyMOL software, the protein is prepared by removing water and other ligands. Afterwards. Using the PyRx Virtual Screening Tool program reduces the Mpro protein energy, and the OpenBabel menu's default settings carry on the process. Open-source programs PyRx and PyMOL can be used to perform docking between ligands and the Mpro protein.

Drug likeness analysis

For additional drug-likeness analysis, the bioactive components of *Illicium verum* were subjected to Lipinski's rule of five using the SCFBIO web server (http://www.scfbio-iitd.res.in/software/drugdesign/lipinski.jsp). It was regarded as a favorable forecast if the two minimal guidelines were observed. The objective of this investigation was to ascertain the pharmacokinetics and likelihood of the medicine molecule candidate passing across the cell membrane if the target was in the cytoplasm.

Molecular docking visualization

The docking data and the 3D structure of the target protein were shown using the PyMOL program. This molecular graphic tool has been widely used to depict 3D pictures of molecules, nucleic acids, proteins, and surfaces (Seeliger & de Groot, 2010). This program was used to create movies and change the annotation of molecules' data. The staining selection was carried out to

distinguish between the target protein's chain domains and the kind of ligands attached, enabling molecular imaging of the 3D protein structure in both animated and surface forms.

Molecular dynamics simulation

Protein modeling is commonly accomplished by molecular dynamic simulation, with CABS-flex as a popular tool. Protein structures with PDB format extensions are needed for CABS-flex. Only single and continuous protein chains are accepted by CABS-flex. The RMSF data and protein simulation will be obtained from the CABS-flex simulation. The documentation on the CABS-flex website is available online and linked to a user email address (Jamroz et al., 2013).

Results and Discussion

The PubChem database provided the chemical compounds in star anise (*Illicium verum*), specifically the inhibitor GC-376, a naturally connected ligand to the Mpro crystal structure. The sample data, which included the 3D structure of the target chemical in.sdf format, was transformed into .pdb format. Consequently, additional analysis might be done using the 3D structure.

On the server (scfbio-iitd.res.in/software/drugdesign/lipinski.jsp), the chemical compounds in star anise are predicted to be drug-like molecules based on Lipinski's rule of five (Saxena et al., 2019). This rule helps distinguish between drug-like and non-drug-like particles based on their essential atomic characteristics. Because of the drug's molecular similarities, Lipinski's rule of five predicts a high probability of success or failure if at least two of the five criteria are met. The rule's requirements are as follows: the molar refractivity must be between 40 and 130, the atomic mass must be less than 500 Da, and the lipophilicity (LogP) of donor hydrogen bonds must be less than 5. These guidelines can help prevent extensive preclinical and late-stage setbacks and aid in early preclinical development (Lipinski, 2004; Jayaram et al., 2012). The results of this investigation demonstrate that Lipinski's rule of five is not broken and that 38 chemical components of star anise are drug-like molecules (Table 1). Consequently, these chemical compounds can proceed to the next level of examination to determine the target protein's binding affinity.

Table 1. Prediction outcomes for drug-like molecules derived from star anise's chemical compounds

Compound Name	Molecular Mass (Da)	Hydrogen Binding Donors	Hydrogen Bond Acceptors	Log P	Molar Refractivity
Cis-anethole	148	0	1	2,728	47.702
Trans-anethole	148	0	1	2,728	47.702
Limonene	136	0	0	3,309	45.912
Linalool	154	1	1	2,670	49.486
Terpinen-4-ol	154	1	1	2,504	47.396
Estragole	148	0	1	2,424	46.895
Anisyl acetone	178	0	2	2,217	51.996
Foeniculin	202	0	1	4,065	66.076
Eucalyptol	154	0	1	2,744	45.527
Trans-linalool oxide	170	1	2	1,881	49.007
Terpinolene	136	0	0	3,453	45.982
Terpinen-1-ol	154	1	1	2,504	47.396
Borneol	154	1	1	2,194	45.236
1,4-cineole	154	0	1	2,744	45.527
Methyl p-anisate	166	0	3	1,481	44.333

To be continued…

4-Methoxy-propiophenone	164	0	2	2,288	47.615
m-Methoxy mandelic acid	182	2	4	0.813	45.59
t-Muurolol	222	1	1	3.776	68.157
4-Ethyl benzaldehyde	134	0	1	2.062	41.207
4-Methoxy benzaldehyde oxime	257	1	4	2.981	73.298
Longifolene	204	0	0	4.415	64.583
3,6-Dimethyl-4H-furo	164	0	3	1.991	41.975
4-Methoxy cinnamaldehyde	162	0	2	1.907	48.092
9-Methyl-9H-fluorene	180	0	0	3.819	59.395
Methylphenyl	381	2	4	4.785	90.319
Bendazol	208	1	1	3.154	65.342
N-(4-hydroxyphenyl)-2-methylbenzamide	227	2	3	2.953	67.239
Phenol-3-[2-(2-phenylethyl)amino]ethyl	241	2	2	2.767	74.826
2-Methyl-3-phenylpropanal	148	0	1	2.064	45.374
Phenyl ethanolamine	137	2	2	1.091	42.017
Surfynol 102	198	2	2	2.092	58.84
Acetic acid geranyl ester	196	0	2	3.241	59.055
Chavicol	134	1	1	2.121	42.008
4-methoxybenzene	108	0	1	1.695	32.994
Nopol	166	1	1	2.361	49.781
3-Undecene	154	0	0	4.313	52.807
Germacrene D	204	0	0	4.891	68.833
Trans-Nerolidol	222	1	1	4.396	72.476
Geranyl isobutyrate	224	0	2	3.878	68.219

Table 2. Results of five *Illicium verum* compounds with the lowest binding affinity

Ligand	Target	Binding Affinity (kcal/mol)	RMSD (Å)
Methylphenyl	Mpro	-9.3	0
4-Methoxy benzaldehyde oxime	Mpro	-8.3	0
N-(4-hydroxyphenyl)-2-methylbenzamide	Mpro	-8.0	0
Bendazol	Mpro	-7.7	0
9-Methyl-9H-fluorene	Mpro	-7.6	0

SARS-CoV-2 Mpro was used as the target in this study, and the chemical components of star anise were used as ligands. The Vina Search Space was maximized in the PyRx program to perform docking simulations for all these compounds, using grid docking centers of X = -15.8898, Y = 30.8037, Z = 11.8171, and dimensions (Å) of X = 67.2857, Y = 92.3790, Z = 97.9206. Molecular docking was used to determine the RMSD value and binding energy. The best RMSD value of the docking study was less than 2 Å. RMSD value is used to predict the quality of contact between the ligand and the protein (Rizvi et al., 2013). Based on the virtual screening findings, methylphenyl was shown to be the chemical molecule in star anise that had the lowest binding energy against

SARS-CoV-2 Mpro (Table 2). A molecular binding experiment was conducted to find molecules, structural elements that differentiate between potential binding modes, and energetic elements that forecast binding scores (Morris & Lim-Wilby, 2008).

The target protein was shown as an animated structure on a transparent surface (Figure 1). The sorts of bonds produced were visualized using the ProteinPlus online site in the PoseView tool, and the chemical combinations with the lowest binding energy were further investigated to ascertain the location of their molecular interactions. Using chemical structure drawing guidelines, the PoseView tool creates 2D representations of complexes with known 3D structures (Stierand et al., 2006). While the interplaying protein residues and ligands were depicted in the structural diagrams, the dashed lines represented the direct bonds between the protein and ligands. Additionally, the hydrophobic regions of the ligands were represented by the spline sections, and the hydrophobic interactions were represented by the communicative amino acids. The 2D drawing program created the structure diagrams and changed their configurations (Fricker et al., 2004). The atom type and a simple built-in interaction model based on geometric criteria were applied to complete the estimates of the interactions between molecules. Methylphenyl compounds engage with hydrogen bonds at His164, Glu166, Gln189, His163, and Phe140 and hydrophobic bonds at His41 and Met165 in the SARS-CoV-2 Mpro domain (Figure 1). The atomically resolved structure at the interface between the ligand and protein is necessary to initiate a new approach to drug design and development. This method used various biophysical elements, including molecular weight, hydrogen bonds, size, hydrophobic interactions, and shape, to maintain atom locations. Reduced intermolecular interactions, such as hydrogen bonding and hydrophobic interactions, maintain the energetically favored ligands in the open conformational environment of protein structures. Tight binding results from prioritizing hydrophobic interactions over hydrogen bonds (Patil et al., 2010).

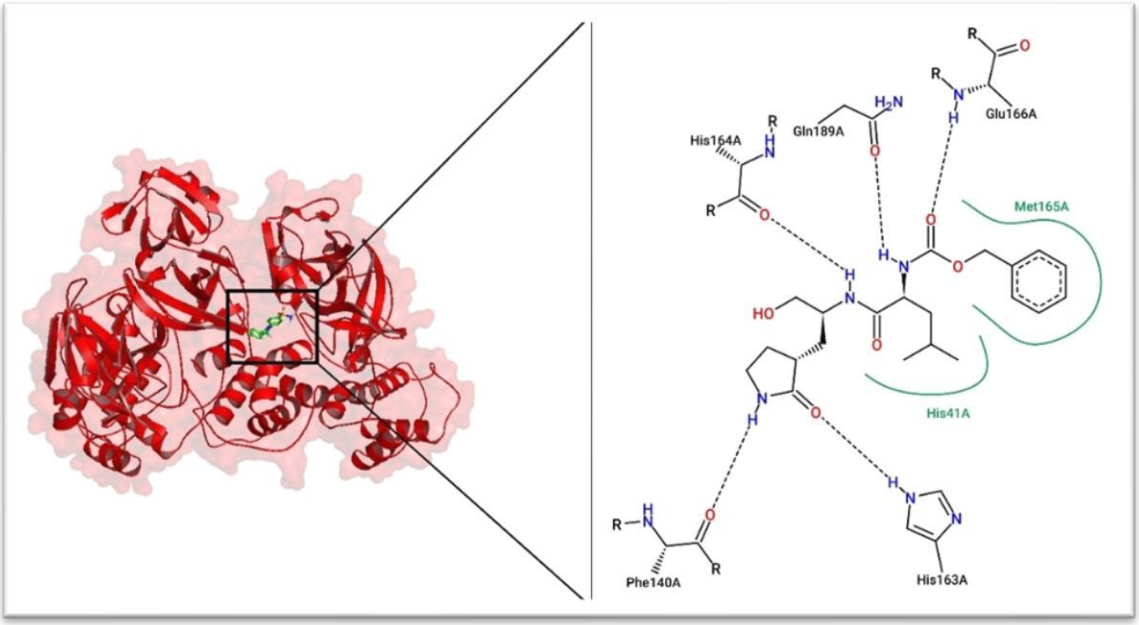

Figure 1. Target Protein Structure (SARS-CoV-2 Mpro) and Methyphenyl Chemical Interactions with it. The SARS-CoV-2 Mpro Target Protein is Visualized with Transparent and Ani-mated Surfaces

The target protein and its ligands are displayed in a 3D structure in Figure 2, along with 2D fluctuation plots. The residue-by-residue changes seen during the simulation are displayed in the fluctuation plot. Plotting multichain proteins involves plotting each chain separately. Only the plot from Chain B is shown because these ligands are linked. The plot's y-axis displays the amino acid

residue index, while the plot's x-axis displays the RMSF values (Å). Conformation will alter the kinetics and flexibility of proteins, as Figure 2 illustrates. Methylphenyl has the lowest free energy, and its protein fluctuation stays below the RMSF criteria of 1-3 Å, according to molecular docking studies using Mpro. As a result, methylphenyl 's structure is regarded as stable.

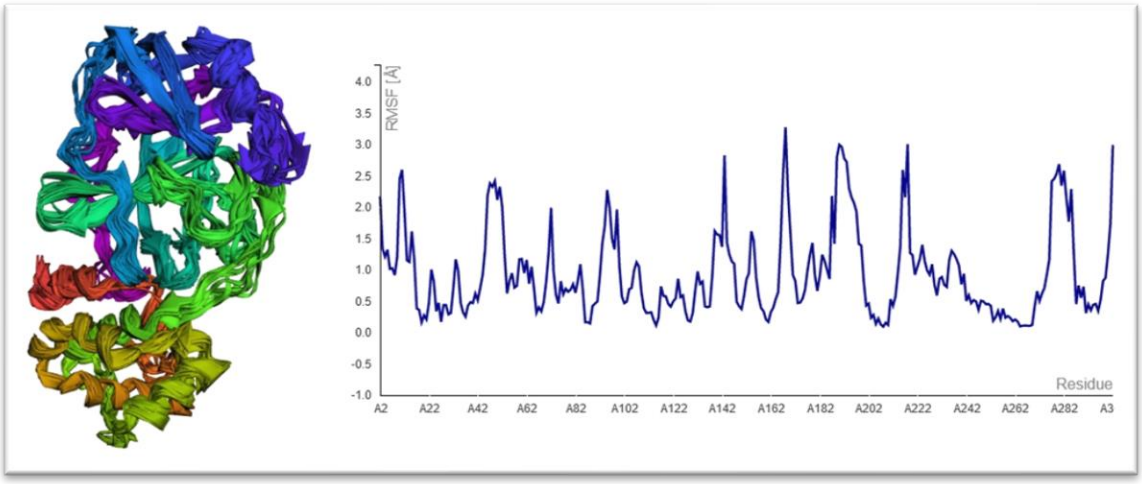

Figure 2. SARS-CoV-2 Mpro's 3D structure and fluctuation plot using methylphenyl (CABS-flex)

All living forms have cycles, and all cycles depend on protein-ligand interactions. All living things are based on atomic complementarity, which is the mechanism by which the ligand mediates signal transmission. Subatomic biological recognition is one of these material responses. The formation of specific spots meant to bind tiny molecule ligands with affinities according to the needs of the cell is partially responsible for the augmentation of proteins (Dunn, 2010). Methylphenyl may bind to SARS-CoV-2 Mpro with the lowest binding energy and interact with the virus through hydrophobic and hydrogen interactions, making it a potential option for drug research and development to treat COVID-19 (Figure 2). Methylphenyl, with an atomic mass of 381 Da, a logP of 4.785, two hydrogen bond donors, four hydrogen bond acceptors, and a molar refractivity of 90.319 (Table 1), also meets Lipinski's rule of five and is classified as a drug-like molecule.

According to molecular dynamics simulations, methylphenyl may be able to interact with SARS-CoV-2 Mpro more successfully, suggesting that it may be used therapeutically to treat SARS-CoV-2 infections by inhibiting Mpro, which will cause it to become inactivated and ultimately fail to assemble virion. Annotations from the thorough virtual screening revealed that chemicals made from star anise are the best candidates. This highlights *Illicium verum*'s bioactive chemicals' apparent reusability as SARS-CoV-2 Mpro inhibitors. It is highly suggested that both in vitro and in vivo investigations be conducted to evaluate the therapeutic efficacy of the previously described experimentally created ligands before conducting clinical trials.

Conclusion

Using Mpro as the SARS-CoV-2 protein target, the star anise bioactive chemicals were tested using techniques, including Lipinski's rule of five, molecular docking analysis, molecular dynamics simulations, and chemical interaction assessment. Molecular docking research and molecular dynamics simulations showed methylphenyl as the most stable ligand. Using the database, more research is advised to find the best formula, especially in pathway prediction. In vitro and in vivo tests are required to demonstrate the potential of methylphenyl. Consequently, spices, including star anise, have bioactive ingredients. Analyses might be carried out to identify which atoms from the protein and ligand bonded to confirm this research further.

Acknowledgment

The authors acknowledge the Mitra Buana Institute of Health and the Hermina Institute of Health, particularly the Department of Research and Community Service (LPPM), for supporting this work.

References

Ansori, A. N. M., Kharisma, V. D., Muttaqin, S. S., Antonius, Y., & Parikesit, A. A. (2020). Genetic variant of SARS-CoV-2 isolates in Indonesia: Spike glycoprotein gene. *J Pure Appl Microbiol.,14*(1), 971-78.

Chen, X., Chen, Y., Yin, Z., Wang, R., Hu, H., Liang, X., He, C., Yin, L., Ye, G., Zou, Y., Li, L., Tang, H., Jia, R., Song, X. (2021). Kaempferol inhibits pseudorabies virus replication in vitro through regulation of MAPKs and NF-κB signaling pathways. 2021. *J. Integr. Agric., 20*, 2227–39.

Dunn, M. F. (2010). Protein-ligand interactions: General description. *Ency. Life Sci.,* https://doi.org/10.1002/9780470015902.a0001340.pub2.

Earlia, N., Suhendra, R., Amin, M., Prakoeswa, C. R. S., & Idroes, R. (2019). GC/MS analysis of fatty acids on pliek U oil and its pharmacological study by molecular docking to filaggrin as a drug candidate in atopic dermatitis treatment. *The Scientific World Journal,* 7. https://doi.org/10.1155/2019/8605743

Fricker, P., Gastreich, M., & Rarey, M. (2004). Automated drawing of structural molecular formulas under constraints. *J Chem. Inf. Comput. Sci., 44,* 1065–78, https://doi.org/10.1021/ci049958u.

Jamroz, M., Kolinski, A., Kmiecik, S. (2013). CABS-flex: server for fast simulation of protein structure fluctuations. *Nucleic Acids Res., 41*(W1), W427-31.

Jayaram, B., Singh, T., Mukherjee, G., Mathur, A., Shekhar, S., Shekhar, V. (2012). Sanjeevini: A freely accessible web-server for target directed lead molecule discovery. *BMC Bioinformatics, 13*(S17). https://doi.org/10.1186/1471-2105-13-s17-s7.

Kandeel, M., & Al-Nazawi, M. (2020). Virtual screening and repurposing of FDA approved drugs against COVID-19 main protease. *Life Sci., 251,* 117627. https://doi.org/10.1016/j.lfs.2020.117627

Kocaadam, B., & Şanlier, N. (2017). Curcumin, an active component of turmeric (*Curcuma longa*), and its effects on health. *Crit Rev Food Sci Nutr., 57*(13), 2889-95.

Liguori, N., Croce, R., Marrink, S. J., & Thallmair, S. (2020). Molecular dynamics simulations in photosynthesis. 2020. *Photosynthesis Res., 144*(2), 273-95.

Lipinski, C. A. (2004). Lead-and drug-like compounds: The rule-of-five revolution. *Drug Discov. Today Technol., 1*(4), 337–341, https://doi.org/10.1016/j.ddtec.2004.11.007.

Morris, G. M., Lim-Wilby, M. (2008). *Molecular docking*. In Kukol, A. (eds.), Molecular Modeling of Proteins., Humana Press, New York. pp. 365–82.

Patil, R., Das, S., Stanley, A., Yadav, L., Sudhakar, A., & Varma, A. K. (2010). Optimized hydrophobic interactions and hydrogen bonding at the target-ligand interface leads the pathways of drug-designing. *PLoS One, 5*(8), e12029, https://doi.org/10.1371/journal.pone.0012029.

Patra, J. K., Das, G., Bose, S., Banerjee, S., Vishnuprasad, C. N., Rodriguez-Torres, M. P., & Shin, H. S. (2020). Star anise (*Illicium verum*): Vhemical compounds, antiviral properties, and clinical relevance. *Phytother Res., 34*(6), 1248-1267. doi: 10.1002/ptr.6614.

Rizvi, S. M. D., Shakil, S., & Haneef, M. (2013). A simple click by click protocol to perform docking: AutoDock 4.2 made easy for non-bioinformaticians. *EXCLI J., 12,* 831.

Saxena, G., Akhtar, S., Sharma, N., Sharma, M., Siddiqui, M. H. A., & Khan, M. K. (2019). Virtual screening, docking and molecular dynamics simulation of selected phytochemical compounds bound to receptor tyrosine kinases: A correlative anti angiogenic study. *Bioinformation, 15*(9), 613–20, https://doi.org/10.6026/97320630015613

Seeliger, D., & de Groot, B. L. (2010). Ligand docking and binding site analysis with PyMOL and Autodock/Vina. *J. Comput. Aided Mol. Des., 24*(5), 417–22, https://doi.org/10.1007/s10822-010-9352-6.

Shaghaghi, N. (2020). *Molecular docking study of novel COVID-19 protease with low risk terpenoids compounds of plants.*

Stierand, K., Maaß, P., & Rarey, M. (2006). Molecular complexes at a glance: Automated generation of two-dimensional complex diagrams. *Bioinformat., 22,* 1710–6, https://doi.org/10.1093/bioinformatics/btl150.

ul Qamar, M. T., Alqahtani, S. M., Alamri, M. A., & Chen, L. L. (2020). Structural basis of SARS-CoV-2 3CLpro and anti-COVID-19 drug discovery from medicinal plants. *J Pharma Analysis, 10*(4), 313-9. https://doi.org/10.1016/j.jpha.2020.03.009

Umesh, H. R., Ramesh, K. V., Devaraju, K. S. (2020). Molecular docking studies of phytochemicals against trehalose–6–phosphate phosphatases of pathogenic microbes. *Beni-Suef Univ J Basic Appl Sci., 9*(1), 1-14.

Zhang, L., Lin, D., Sun, X., Curth, U., Drosten, C., Sauerhering, L., Hilgenfeld, R. (2020). Crystal structure of SARS-CoV-2 main protease provides a basis for design of improved α-ketoamide inhibitors. *Science, 368*(6489), 409-12.